Bertrand Georgeot

Quantware group, Lab. de Physique Théorique, UMR 5152 du CNRS

Université Paul Sabatier, Toulouse, France www.quantware.ups-tlse.fr

Acknowledgments: Dima Shepelyansky (researcher CNRS), Daniel Braun (University Paul Sabatier), Olivier Giraud (researcher CNRS), Marcello Terraneo (former postdoc) Benjamin Lévi (former PhD student)

SUPPORT: IST-FET (EU), ANR (France)

Lectures by B. Georgeot 1-2

Institut Henri Poincaré

Trimester at Centre Émile Borel

Quantum Information, Computation and Complexity

Bertrand Georgeot

CNRS and Université Paul Sabatier, Toulouse, France

Quantum computation and complex dynamics

Lectures by B. Georgeot 1-2: overview

1) Classical and quantum chaos

2) Simulation of quantum chaos maps on quantum computers

3) Extracting information from quantum simulations

4) Simulation of classical chaos on quantum computers

Classical integrable systems

- Systems with as many **constant of motion** $I_1, ..., I_n$ as degrees of freedom
- There exists a (canonical) change of variables to **action-angle** variables such that Hamilton's equations of motion become: $\dot{I}_i = 0, \dot{\theta}_i = \omega_i$
- Motion takes place on n-dimensional **tori** in a $2n$-dimensional phase space
- Tori can be rational or irrational
- One degree of freedom: integrable system if energy is conserved
- Examples: square billiard, circular billiards, two-body Kepler problem ...

Classical chaos

- No constant of motion $\Rightarrow$ motion not restricted to tori.
- Lowest degree of chaos: **Ergodic** motion: most trajectories fill up the energy shell.
- Next levels (ergodic hierarchy): mixing, K-systems, Bernoulli systems
- **Hard chaos**: exponential separation of nearby trajectories ($\Rightarrow$ exponential sensitivity to initial conditions)
- Famous examples of chaotic systems: Sinai billiard, Bunimovich billiard (stadium), three-body Kepler problem...

Mixed systems

- Most systems have integrable and chaotic zones: **mixed systems**
- Kolmogorov-Arnold-Moser (KAM) theorem: (smooth) perturbation of integrable systems keeps aspects of integrability and leads to mixed systems
- Result of KAM theory: rational tori disappear as soon as the perturbation is nonzero, and are replaced by chains of integrable islands (resonances) surrounded by chaotic layers
- Result of KAM theory: irrational tori survive for nonzero perturbation and form a set of nonzero measure in phase space. They are first deformed and finally disappear for stronger perturbation.

Chaotic maps

- Simplest systems: **one-dimensional systems** (phase-space of dimension 2) $\Rightarrow$ needs time-dependence to allow chaotic dynamics

- Example: $H(I,\theta,t) = I^2/2 + kV(\theta)\sum_m \delta(t-mT)$, where θ is a phase and I corresponds to classical action. Phase space=cylinder (θ in $[0,2\pi]$). Free rotation, with a "kick" every period.

- Integration over one period $\Rightarrow$ area-preserving map with discretized time $\bar{I} = I - kV'(\theta);\ \bar{\theta} = \theta + T\bar{I}$ (bars denote values of (I,θ) after one iteration)

- For many choices of V, dynamics becomes chaotic when $K = kT$ increases.

- Many complex phenomena present in physical systems can be studied in such models, despite simplicity.

Example: Chirikov standard map

If $V(\theta) = \cos(\theta)$; the map is $\bar{I} = I + k \sin\theta$; $\bar{\theta} = \theta + T\bar{I}$ with $(I, \theta) =$ conjugated momentum (action) and angle variables,

- dynamics on a cylinder (periodicity in θ), controlled by a single parameter $K = kT$.
- $K = 0 \Rightarrow$ system is integrable, all trajectories lie on one-dimensional tori ($n =$constant).
- $K > 0 \Rightarrow$ transition to chaos (KAM theorem).

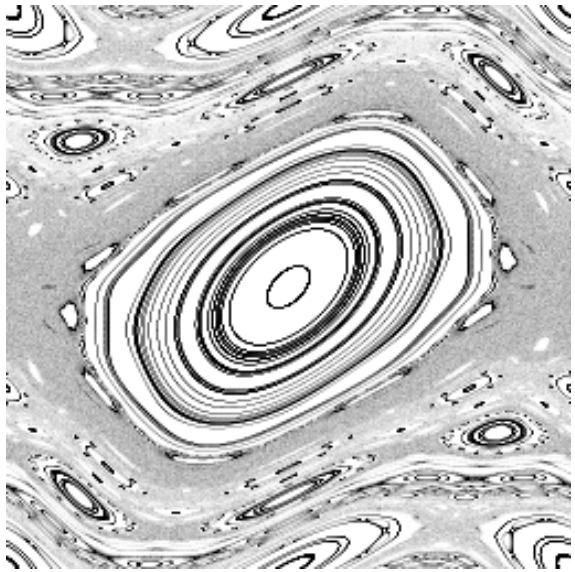

classical phase space at $K = K_g = 0.9716...$

Transport in Chirikov standard map

- As long as irrational tori are present, they prevent transport through them and the onset of global chaos
- $K > K_g \approx 0.9716... \Rightarrow$ last torus disappears $\Rightarrow$ global chaos, classical diffusion
- Diffusion rate $D = \langle I^2 \rangle / t \approx k^2/2$

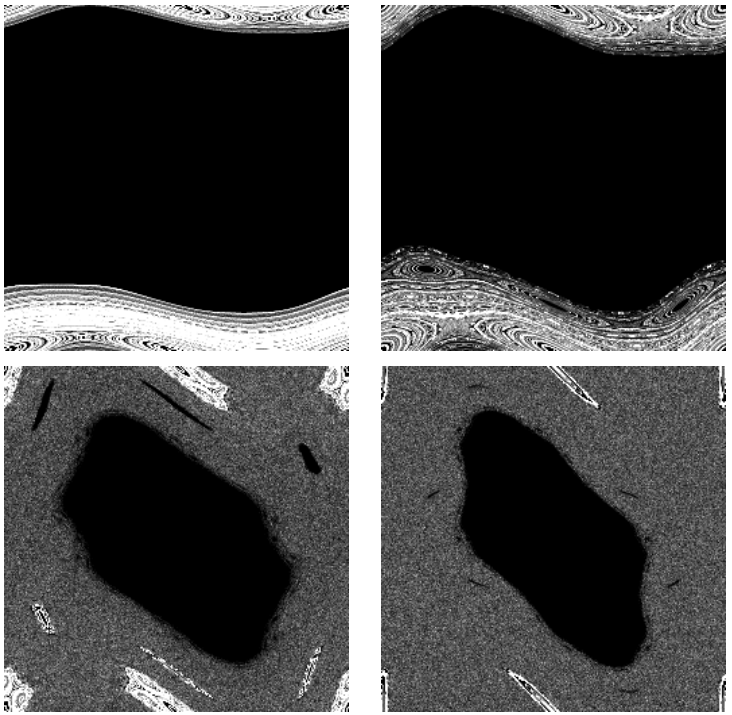

transport at $K = 0.5, 0.9, 1.5, 2$

Quantum chaos

- Quantum mechanics is the "true" mechanics $\Rightarrow$ what corresponds to chaotic properties of classical physics?
- Schroedinger equation is **linear**, principle of superposition $\Rightarrow$ hard to find exponential separation in quantum mechanics
- Intrinsic scale $\hbar$, non commutativity of p and q
- Classically integrable systems $\Rightarrow$ wave functions **localized** in phase space on quantized tori
- Classically chaotic systems $\Rightarrow$ wave functions usually **ergodic**
- Mixed systems show aspects of both quantum properties

Semiclassical limit

- Quantum mechanics can be obtained from classical mechanics for small $\hbar$ (i.e. $\hbar$ is small compared to quantities of same dimension (=actions) in the system) $\Rightarrow$ **semiclassical approximation**

- For integrable systems, EBK formulas give semiclassical approximation for energies, wavefunctions in term of individual torus

- 1970's: Gutzwiller, Balian and Bloch: **trace formulas** to connect quantum observables to a set of classical trajectories (Fourier-like formulas)

Random Matrix Theory

- Wigner 1960's: statistical properties of neutron scattering experiments on nuclei $\Rightarrow$ Replace complex Hamiltonian by **large random matrix** with Gaussian distributed entries.

- **Density of states** $d(E) \Rightarrow$ **Mean value** usually system-dependent. **Fluctuations** of energy levels around mean position: good agreement between nuclear experiments and Random Matrices, despite **no adjustable parameter**.

- Bohigas Giannoni Schmit (1984): Random Matrix Theory should describe statistical properties of spectra of **classically chaotic systems** (conjecture). Conjecture verified on numerous examples, but unproven

- Berry-Tabor (1977): for integrable systems, statistical properties of spectra are **Poissonian**; i.e. no correlations.

Symmetry considerations

→ Three **different** Random Matrix ensembles:

- Gaussian Unitary Ensemble (GUE): hermitian matrices. Corresponds to systems without time-reversal symmetry.
- Gaussian Orthogonal Ensemble (GOE): real symmetric matrices. Corresponds to systems with time-reversal symmetry.
- Gaussian Symplectic Ensemble (GOE): real quaternionic matrices.

→ Same for **circular ensembles** (evolution operators) CUE, COE, CSE

→ Other symmetries (e. g. spatial symmetries) lead to **independent spectra**

⇒ should separate these spectra to compare with Random Matrix results

Random Matrix Theory: standard quantities

$\longrightarrow$ Correlation function $C(\omega)$

$C(\omega) = \langle d(E)d(E+\omega)\rangle_E$

Form factor $K(t)$

$K(t) = \int \exp(2i\pi\omega t)C(\omega)d\omega$

$\longrightarrow$ Nearest-neighbor distribution $P(s)$ or spacing distribution: **short-range quantity**

Wigner $\Rightarrow$ level repulsion at short distances

$\longrightarrow$ Spectral variance: variance of the number of energy levels in a box of size L (in units of mean level spacing) **long-range quantity**

RMT: $\Sigma_2 \sim \log L$ for large L

Poisson: $\Sigma_2 \sim \sqrt{L}$ for large L

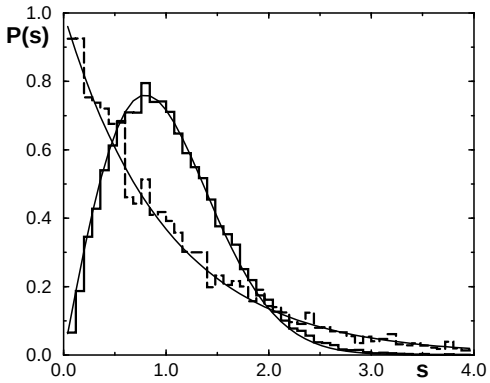

Wigner distribution (GOE):

$P_W(s) = (\pi s/2)\exp(-\pi s^2/4)$

Poisson: $P_P(s) = e^{-s}$

Anderson localization

- P. W. Anderson (1958): in a disordered potential, a quantum particle can be **exponentially localized** due to quantum interferences
- This happens even though the corresponding classical system is diffusive
- **Result:** For localization length smaller than system size, localized states correspond to **Poisson statistics**. Delocalized (ergodic) states in general follow **Random Matrix predictions**.
- In dimension three, presence of a **metal-insulator transition** $\Rightarrow$ can be probed through spectral statistics
- **Quantum chaos can mimic disorder:** in the **kicked rotator** model, localization appears due to quasirandomness of chaos

Quantum maps

Quantization: $\bar{\psi} = U\psi$ where ψ is the wavefunction and $\bar{\psi}$ its new value after one iteration of the evolution operator $U = e^{-ikV(\theta)}e^{-iT\hat{n}^2/2}$. $\hat{n} = -i\partial/\partial\theta$.

Example: kicked rotator: quantization of Chirikov standard map

$$\bar{\psi} = \hat{U}\psi = e^{-ik\cos\hat{\theta}}e^{-iT\hat{n}^2/2}\psi$$

where $\hat{n} = -i\partial/\partial\theta$, and $\psi(\theta + 2\pi) = \psi(\theta)$.

- Quantum dynamics depends on two parameters k and T (classical: one single parameter $K = kT$). T plays the role of an effective $\hbar$
- Classical limit corresponds to $k \to \infty$, $T \to 0$ while keeping $K = kT$ =constant

Transport in quantum kicked rotator

- $K < K_g \approx 0.9716..$: quantum diffusion limited by KAM tori

- $K \gg K_g$: classical diffusion replaced by quantum localization; wave function $\sim \exp(-|n-m|/l)/\sqrt{l}$ with localization length $l = D/2 \approx k^2/4$

- If localization length is greater than system size $\Rightarrow$ Random Matrix Theory, ergodicity

The kicked rotator is a paradigmatic model of quantum chaos, modelizes Rydberg atoms in microwave fields, and enables to study Anderson localization of electrons. It has been experimentally realized with cold atoms

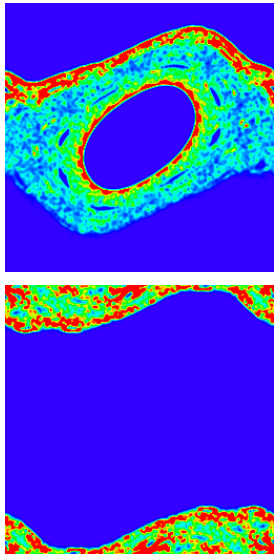

wave packet evolution, $K = K_g$

Quantum phase space distribution function: Wigner function

$$W(p,q) = \frac{1}{\sqrt{2\pi\hbar}} \int e^{-\frac{i}{\hbar}p.q'} \psi(q+\frac{q'}{2})^* \psi(q-\frac{q'}{2}) dq'$$

Real but can take **negative values**

$\int_q W(p,q)dq = |\psi(p)|^2$

$\int_p W(p,q)dp = |\psi(q)|^2$

On a N-dimensional Hilbert space (e. g. kicked rotator): use $2N \times 2N$ points.

$$W(\Theta,n) = \frac{1}{2N} \sum_{m=0}^{N-1} e^{-\frac{2i\pi}{N} n(m-\Theta/2)} \psi(\Theta-m)^* \psi(m)$$

Figure: Wigner function of a wavepacket for kicked rotator, $K = 0.9$ (top), $K = 2$ (bottom).

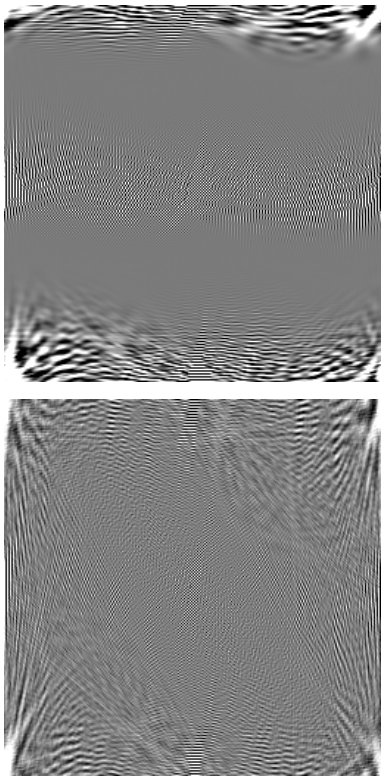

Quantum phase space distribution function: Husimi function

Unlike classical phase space distribution function, Wigner function can be negative. Smoothing of Wigner function over cells of size $\hbar \Rightarrow$ real nonnegative function

Husimi function:

$\rho_H(\theta_0, n_0) = |\langle \phi_{(\theta_0,n_0)} | \psi \rangle|^2$

where $\phi_{(\theta_0,n_0)}(\theta, n) = A \sum_n e^{-(n-n_0)^2/4a^2 - i\theta_0 n} |n\rangle$

Modified Husimi function:

$\rho_H^{(p)}(\theta_0, n_0) = |\langle \phi^{(p)}_{(\theta_0,n_0)} | \psi \rangle|^2$

where $\phi^{(p)}_{(\theta_0,n_0)}(\theta, n) = (1/N^{1/4}) \sum_{n=n_0}^{n_0+\sqrt{N}-1} e^{-i\theta_0 n} |n\rangle$

Figure: Modified Husimi function of a wavepacket for the kicked rotator, $K = 0.9$ (top), $K = 2$ (bottom).

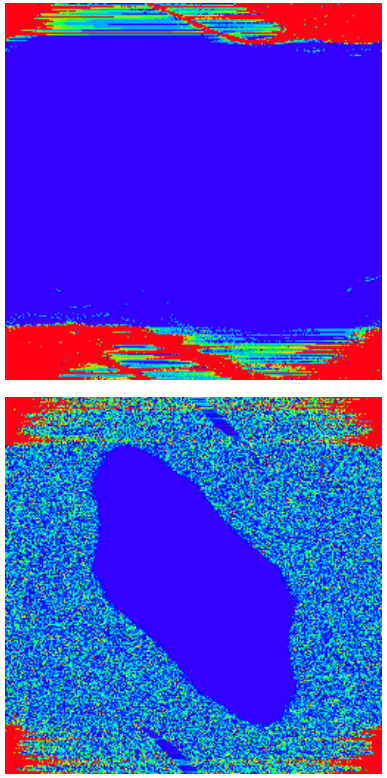

Quantum programming instructions: quantum gates

One acts on the wave function of the quantum computer through **unitary transformation**. In practice, One uses **elementary quantum gates** which are **local** and compose them to build the unitary evolution needed.

- **Hadamard gate** applied to one qubit $|0\rangle \rightarrow (|0\rangle + |1\rangle)/\sqrt{2}$; $|1\rangle \rightarrow (|0\rangle - |1\rangle)/\sqrt{2}$;
- **controlled not** or **CNOT** applied to two qubits: $|00\rangle \rightarrow |00\rangle$; $|01\rangle \rightarrow |01\rangle$;$|10\rangle \rightarrow |11\rangle$; $|11\rangle \rightarrow |10\rangle$; the second qubit is changed if the first is in the state $|1\rangle$;
- **controlled controlled not** or **Toffoli gate** applied to three qubits: the third qubit is changed if the first two are both in the state $|1\rangle$.

Quantum computation of functions

$\Rightarrow \sum_{i=0}^{N-1} \sum_{j=0}^{N-1} a_i |i\rangle |0...000\rangle \Rightarrow \sum_{i=0}^{N-1} a_i |i\rangle |f(i)\rangle$, with f some arithmetical function

$\Rightarrow$ Example: **addition;** a quantum computer needs only $\approx 8n$ quantum gates and $\approx 3n$ qubits to perform N^2 additions reversibly ($N = 2^n$), with one workspace register erased at the end

$\Rightarrow$ **Multiplications and exponentiations** can also be done; it need $\sim n^2$ (multiplication) and $\sim n^3$ quantum gates (exponentiation) for $\sim N$ numbers encoded in n qubits ($N = 2^n$).

$\Rightarrow$ In computational basis, evolution is described by **permutation matrix**

Quantum Fourier Transform

Uses n qubits to transform a vector of size $N = 2^n$ by:

$$\sum_{k=0}^{2^n-1} a_k|k\rangle \longrightarrow \sum_{l=0}^{2^n-1}(\sum_{k=0}^{2^n-1} e^{2\pi ikl/2^n} a_k)|l\rangle = \sum_{l=0}^{2^n-1} \tilde{a}_l|l\rangle \ .$$

Can be written through elementary transformations: H_j : **Hadamard gate** applied to qubit j, and B_{jk}: **two-qubit gate** applied to the qubits j and k, characterised by $|00\rangle \rightarrow |00\rangle$; $|01\rangle \rightarrow |01\rangle$;$|10\rangle \rightarrow |10\rangle$; $|11\rangle \rightarrow \exp(i\pi/2^{k-j})|11\rangle$).

One can verify that the sequence: $\Pi_{j=1}^{n}[(\Pi_{k=j+1}^{n} B_{jk})H_j]$

gives the Fourier transform of a vector of size 2^n in $n(n+1)/2$ operations.

Compare with $\sim N \log N$ for the classical Fast Fourier Transform

Programming a quantum computer

Subroutines

- Quantum addition:
- Quantum multiplication and exponentiation
- Quantum Fourier transform
- Quantum wavelet transform

Known algorithmic tools

- Period finding aka hidden subgroup
- Grover's search of an unstrucured database
- Amplitude amplification
- Phase estimation
- Quantum counting

Simulation of quantum physical systems

Motivation: Many quantum mechanical problems require **large** Hilbert spaces. Examples: many-body systems (n particles, m orbitals $\Rightarrow m^n$ states), semiclassical limit... A lot of computer time is devoted to such simulations in modern times

History

- Feynman (1982): Use quantum mechanical systems to simulate quantum mechanics
- Lloyd (1996), Abrams and Lloyd (1997): algorithms to simulate many-body systems with local interactions.
- Wiesner (1996), Zalka (1998): algorithms simulating Schroedinger equation

Quantum maps are **especially simple** systems with **complex dynamics**

Simulation of quantum maps: baker's map

R. Schack Phys. Rev. A 57, 1634 (1998)

- Classical: $(q,p) \to (2q, \frac{p}{2})$ for $0 \leq q \leq \frac{1}{2}$; $(q,p) \to (2q-1, \frac{p+1}{2})$ for $\frac{1}{2} < q \leq 1$
- Quantum: define F_n $N \times N$ matrix with $N = 2^n$ by $(F_n)_{kj} = \frac{e^{-\frac{2i\pi kj}{N}}}{N}$. Then evolution operator on a N-dimensional space, $N = 2^n$ is $F_n^{-1} \begin{pmatrix} F_{n-1} & 0 \\ 0 & F_{n-1} \end{pmatrix}$
- F_n=discrete Fourier transform $\Rightarrow$ Quantum Fourier transform $\Rightarrow$ can be implemented with $n(n-1) + n(n+1)/2 = n(3n-1)/2$ quantum gates.
- Implemented on a NMR quantum computer with 3 qubits **(Y. S. Weinstein, S. Lloyd, J. Emerson, and D. G. Cory, Phys. Rev. Lett. 89, 157902 (2002))**.

Simulating the kicked rotator

B. Georgeot and D. Shepelyansky, Phys. Rev. Lett. 86, 2890 (2001)

On a Hilbert space of dimension $N = 2^{n_q}$:

classical computation: one iteration $\Rightarrow O(N \log N)$ operations

quantum computation: one iteration $\Rightarrow O((\log N)^3)$ quantum gates

Two regimes:

a) k and T constant, N increases $\Rightarrow$ number of cells increases, with fixed number of states per cell (localization visible)

b) $T \propto 1/N$ and $K = kT$ constant, N increases $\Rightarrow$ number of cells fixed, number of states per cell increase (semiclassical limit visible)

Quantum algorithm for simulation of kicked rotator I

- **Step I** preparation of initial state: $\psi(0) = \sum_{p=0}^{N-1} a_n |n\rangle$; For example $\psi(0) = |N/2\rangle$

- **Step II** action of $e^{-iT\hat{n}^2/2}$: $\sum_{n=0}^{N-1} a_n |n\rangle \Rightarrow \sum_{n=0}^{N-1} a_n e^{-iTn^2/2} |n\rangle$

  (by $n_q^2 = (\mathrm{Log}_2(N))^2$ applications of two-qubit gates)

- **Step III** quantum Fourier transform: $\sum_{p=0}^{N-1} a'_n |n\rangle \Rightarrow \sum_{i=0}^{N-1} b_i |\theta_i\rangle$ with $b_j = \frac{1}{N} \sum_{n=0}^{N-1} a'_n e^{2i\pi jn/N} \Rightarrow$ change from n to θ representation

Quantum algorithm for simulation of kicked rotator II

- **Step IV** construction of the cosines: $\sum_{i=0}^{N-1} b_i|\theta_i\rangle|0\rangle \Rightarrow \sum_{i=0}^{N-1} b_i|\theta_i\rangle|\cos\theta_i\rangle$
  (needs $\sim n_q^3$ gates;)

- **Step V** action of $e^{-ik\cos\hat{\theta}}$: $\sum b_i|\theta_i\rangle|\cos\theta_i\rangle \Rightarrow \sum b_i e^{-ik\cos\theta_i}|\theta_i\rangle|\cos\theta_i\rangle$
  (by $n_q = (\mathrm{Log}_2(N))$ applications of one-qubit gates)
  Then $\sum_{i=0}^{N-1} b'_i|\theta_i\rangle|\cos\theta_i\rangle \Rightarrow \sum_{i=0}^{N-1} b'_i|\theta_i\rangle|0\rangle$ (erasing the cosines)

- **Step VI** quantum Fourier transform: $\Rightarrow$ back to n representation

Total complexity: $O((\log N)^3)$ quantum gates; needs only $\sim \log N$ qubits

Quantum algorithm for simulation of sawtooth map

G. Benenti, G. Casati, S. Montangero and D. L. Shepelyansky, Phys. Rev. Lett. 87, 227901 (2001)

$\bar{I} = I + k(\theta - \pi); \quad \bar{\theta} = \theta + T\bar{I}$

$\bar{\psi} = U\psi$ with the evolution operator

$U = e^{-iT\hat{n}^2/2} e^{ik(\hat{\theta}-\pi)^2/2}$.

On a Hilbert space of dimension $N = 2^{n_q}$:

Same as above but crucially Steps IV and V (action of $e^{-ik\cos\hat{\theta}}$) replaced by much simpler action of $e^{ik(\hat{\theta}-\pi)^2/2}$: $\sum b_i|\theta_i\rangle \Rightarrow \sum b_i e^{ik(\hat{\theta}-\pi)^2/2}|\theta_i\rangle$

(by $n_q^2 = (\mathrm{Log}_2(N))^2$ applications of two-qubit gates)

In total needs only $3n_q^2 + n_q$ quantum gates per iteration and uses no workspace qubit.

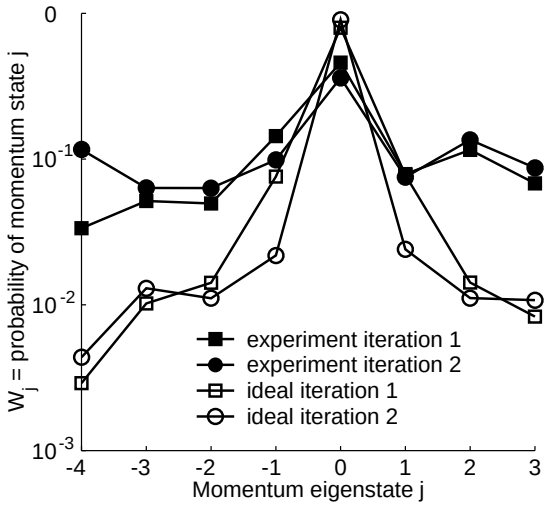

Experimentally implemented with three qubits with NMR technique **(M. Henry, J. Emerson and D. Cory, quant-ph 0512204)**.

Anderson transition map

- Kicked rotator and sawtooth map have **localized** states for K large enough. Physical system can also display an **Anderson metal-insulator transition**

- Can be realized in a **generalized kicked rotator model** described by

  $\bar{\psi} = \hat{U}\psi = e^{-iV(\theta,t)}e^{-iH_0(n)}\psi$

  with $V(\theta,t) = k[1 + 0.75\cos(2\pi t/\lambda)\cos(2\pi t/\lambda^2)]\cos\theta$ with $\lambda = 1.3247...$

  and $H_0(n)$ random phases distributed in $(0, 2\pi)$

  $\Rightarrow$ **Anderson transition** at $k_c \approx 1.8$ between **localized** and **extended** states

- Simulation of N-dimensional wave function can be realized in $O((\log N)^2)$ operations **(A. Pomeransky and D. Shepelyansky, Phys. Rev. A 69, 014302 (2004)).**

Kicked Harper model

B. Lévi and B. Georgeot Phys. Rev. E 70, 056218 (2004)

$\bar{n} = n + K \sin\theta$, $\bar{\theta} = \theta - L \sin\bar{n}$

Transition to chaos as K, L increase

Quantization: $\bar{\psi} = e^{-iL\cos(\hbar\hat{n})/\hbar} e^{-iK\cos(\hat{\theta})/\hbar}\psi$

$K = L \to 0$ gives Harper model with **fractal spectrum**

dynamical localization $\to$ similar to Anderson localization of electrons in solids

transition to a **partially delocalized regime**, with coexistence of localized and delocalized states

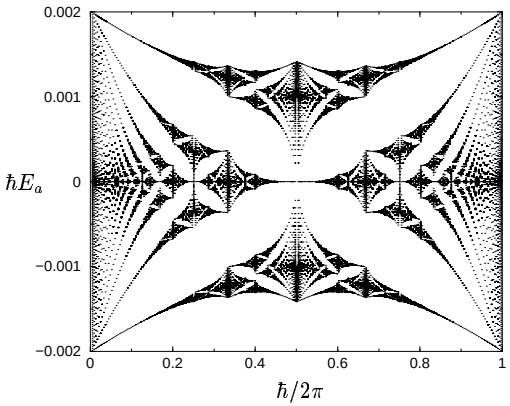

spectrum for $K, L \Rightarrow 0$

On a N dimensional Hilbert space with $N = 2^{n_q} \Rightarrow$ Exact algorithm (cf kicked rotator): needs $O(\log N^3)$ quantum gates for evolution of the wave function + workspace registers

Implementing $e^{-ik\cos(p\,\hat{\theta})}$: time-slice algorithm

(cf A. A. Pomeransky and D. L. Shepelyansky, Phys. Rev. A 69, 014302 (2004).)

$M(\alpha,U) = HC_UHe^{i\frac{\alpha}{2}\sigma_z}HC_{U^{-2}}He^{i\frac{\alpha}{2}\sigma_z}HC_UH$ (C_U is U controlled by ancilla)

One has $M(\alpha,U) = 1 + i\alpha\frac{U+U^{-1}}{2} + O(\alpha^2)$

For $U = e^{ip\theta}$ then $M(\alpha,U) = 1 + i\alpha\cos(p\,\theta)\sigma_z + O(\alpha^2) \approx e^{i\alpha\cos(p\,\hat{\theta})}$

Thus $e^{-ik\cos(p\,\hat{\theta})} \approx M(\alpha,U)^{n_s}$ with $\alpha = \frac{-k}{n_s}$ and error $O(\alpha^2)$

Symmetrization: $\widetilde{M}(\alpha,U) = M\left(\frac{\alpha}{2},U\right)M\left(\frac{\alpha}{2},U^{-1}\right) \Rightarrow$ error $O(\alpha^3)$

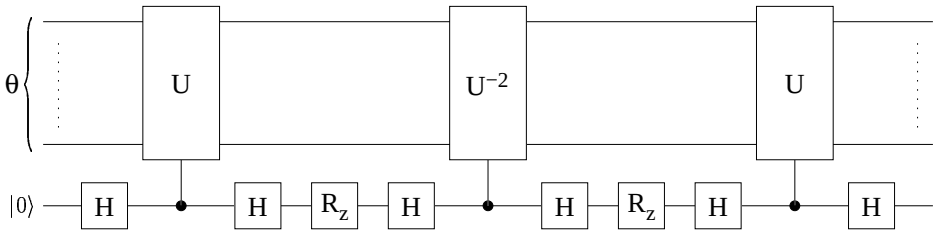

Kicked Harper model: time-slice algorithm

For kicked Harper model on $N = 2^{n_q}$-dimensional space: $e^{-iK\cos(\hat{\theta})/\hbar}$ and $e^{-iL\cos(\hbar\hat{n})/\hbar} \Rightarrow 4 + 2(n_q - a) + (n_s - 1)(7 + 2(n_q - a))$ gates

QFT $\Rightarrow n_q^2$ gates

Only one ancilla qubit! $O(\log N)^2$ quantum gates

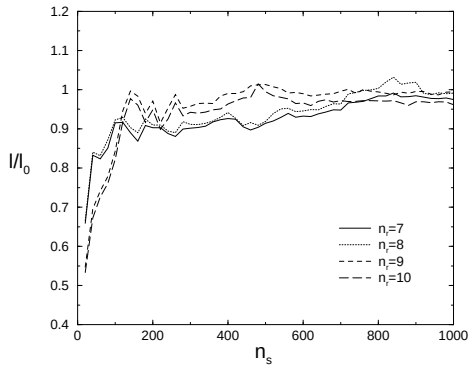

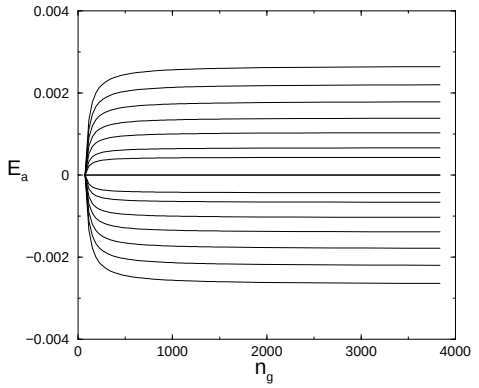

Numerics: localization length eigenphases

Kicked Harper: Chebychev polynomials algorithm

$$T_0(x) = 1, \quad T_1(x) = x, \quad T_n(x) = 2xT_{n-1}(x) - T_{n-2}(x)$$

Let us take $f(x)$ a function on $[-1, 1]$, and $c_j = \frac{2}{M} \sum_{k=0}^{M-1} f\left[\cos\left(\frac{\pi\left(k+\frac{1}{2}\right)}{M}\right)\right] \cos\left(\frac{\pi j\left(k+\frac{1}{2}\right)}{M}\right) \Rightarrow$ for large M, $\sum_{j=0}^{M-1} c_j T_j(x) - \frac{1}{2}c_0$ is a **very good approximation** of $f(x)$ on $[-1, 1]$.

$$P(x) \approx \cos\left(\pi(x+1)\right) \Rightarrow e^{-ik\cos\left(p\,\hat{\theta}\right)} \approx e^{-ikP\left(\frac{p\hat{\theta}}{\pi}-1\right)}$$

Chebychev polynomial approximation of degree $d \Rightarrow$ **complexity is** $O({n_q}^d)$. Numerics: $d = 6 \Rightarrow$ very good approximation of the wave function. $(N = 2^{n_q})$

Dropping the gates with the **smallest phases** shortens the computation.

No ancilla qubit! $O(\log N)^d$ quantum gates

Problem of extraction of information

- Several quantum maps can be **efficiently simulated** on a quantum computer, using polynomial resources to simulate exponentially large Hilbert spaces
- Many **complex phenomena** present in physical systems can be studied through such maps
- Such maps can be implemented in some cases in **present day quantum computers**
- Yet to have a complete quantum algorithm, and assess efficiency, one needs to take into account the **measurement process** after producing the final wavefunction
- **How to extract efficiently information from a complex wavefunction?**

Simple approach: coarse grained measurements

- Measure only the first n_f qubits $\longrightarrow$ polynomial number of measurements gives **coarse grained image** of the wave function
- Possibility of exponential gain
- But polynomial approximation of wavefunction $\Rightarrow$ should be compared to other approximations
- Also, quantum wave packets have to spread enough time to get useful information $\Rightarrow$ may make the gain much smaller

Localization length

Kicked rotator, sawtooth map and other models present **localized states**. Localization length l **measured directly** by fitting an exponential function around maximal values of ψ, obtained by **coarse grained measurements** $\Rightarrow$ **effective, no extra cost (G. Benenti, G. Casati, S. Montangero and D. L. Shepelyansky, Phys. Rev. A 67, 052312 (2003))**

But needs to **evolve wave function** until size $\approx l \approx D$ (D is diffusion constant). Short time $\Rightarrow$ diffusive spreading $\langle n(t)^2 \rangle \approx Dt$; thus wave packet needs to be evolved until time $t^* \approx l^2/D \approx l$

Classically: to evolve a vector of dimension $\sim l$ for time $t^* \Rightarrow \sim l^2$ operations.

Quantum computer: total number of gates $\sim l$.

$\Rightarrow$ quadratic improvement for the quantum algorithm.

Transport properties

Example: kicked Harper model in partially delocalized regime: Coexistence of localized and delocalized wave functions; wave packet = localization peak + delocalization plateau; **extraction of diffusion constant (of the plateau)**

a) away from $K = L$ line: anomalous diffusion (ballistic)

$\Rightarrow$ time evolution up to time t^*: $\sim (t^*)^2$ operations classically, $\sim t^*$ quantum

b) on the $K = L$ line: normal diffusion

$\Rightarrow$ time evolution up to time t^*: $\sim (t^*)^{3/2}$ operations classically, $\sim t^*$ quantum

$\Rightarrow$ polynomial improvement for the quantum algorithm.

Larger gain for systems where spreading of wavepacket is faster (e. g. quantum small-world networks where the gain is possibly exponential).

Measuring the fidelity decay

J. Emerson, Y. S. Weinstein, S. Lloyd and D. Cory, Phys. Rev. Lett. 89, 284102 (2002)

- Needs a quantum map with evolution operator U efficiently implementable on QC + a perturbed evolution operator U_p also efficiently implementable
- Fidelity is $F(t) = |\langle U^t \psi_0 | U_p^t \psi_0 \rangle|^2$ where $\psi_0 = U_0|0\rangle$=initial state
- Then $\langle U^t \psi_0 | U_p^t \psi_0 \rangle = \langle 0 | U_0^+ (U^+)^t U_p^t U_0 | 0 \rangle$
- **Simulating** $U_0^+ (U^+)^t U_p^t U_0$ and **sampling** population of the state $|0\rangle$ gives the **fidelity**
- **Possible exponential gain**

Experiment on the fidelity decay

C.A. Ryan, J. Emerson, D. Poulin, C. Negrevergne, R. Laflamme, 2005

	C_1	C_2	C_3	C_4	M	H_1	H_2
C_1	−2972						
C_2	40.5	−25518					
C_3	1.5	69.9	−21583				
C_4	7.1	1.4	72.4	−29544			
M	127.5	−7.1	6.6	−0.9	−1292		
H_1	3.8	156.0	−1.8	6.5	6.9	−4855	
H_2	6.2	−0.7	162.9	3.3	−1.7	15.5	−4066

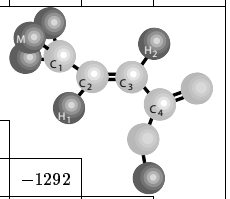

molecule

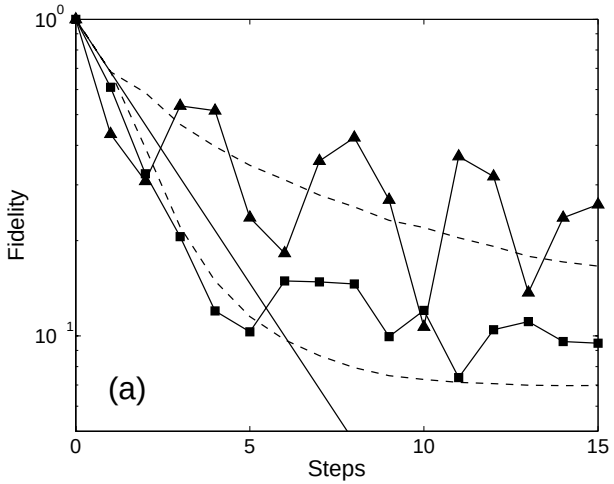

regular regime

fluctuations

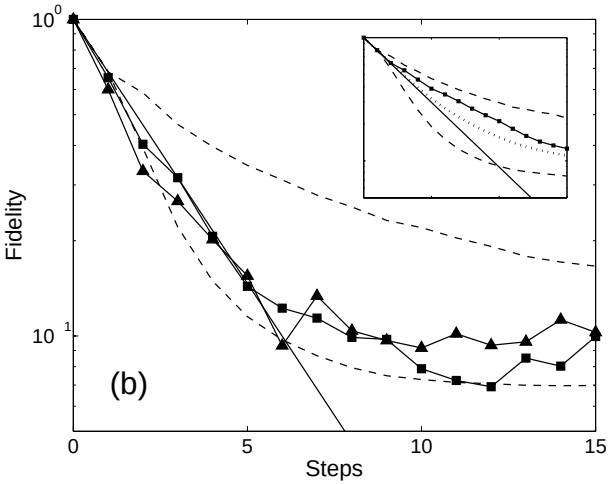

complex map

universality

Measuring the form factor

D. Poulin, R. Laflamme, G. J. Milburn and J. P. Paz, Phys. Rev. A 68, 022302 (2003)

Needs an evolution operator U efficiently simulated on quantum computer

Uses one ancilla qubit on which the value of the **traces** are transfered ("scattering circuit"). $\mathrm{Tr}U^p/N = \langle\sigma_z\rangle$ for the probe qubit. For quantum maps, $< \mathrm{Tr}U^p >_p$ gives form factor $K(t)$. Value of form factor near $t = 0 \Rightarrow$ **characterizes Random Matrix , Poisson and intermediate statistics** (the latter can be probed in e. g. the map $\hat{U} = e^{-2i\pi\hat{p}^2/N}e^{2i\pi\alpha\hat{q}}$)

$\rightarrow$ If $< \mathrm{Tr}U^p >_p \sim \kappa\sqrt{N}$ then $K(0) = |\kappa|^2$ and statistics are integrable ($|\kappa|^2 = 1$) or intermediate ($|\kappa|^2 < 1$)

$\rightarrow$ If $< \mathrm{Tr}U^p >_p \sim 1$ then $K(0) = 0$ (Random Matrix statistics)

Quadratic gain compared to classical computation

Wigner function

On a N-dimensional Hilbert space: use $2N \times 2N$ points.

$$W(\Theta, n) = \frac{1}{2N} \sum_{m=0}^{N-1} e^{-\frac{2i\pi}{N} n(m-\Theta/2)} \psi(\Theta - m)^* \psi(m)$$

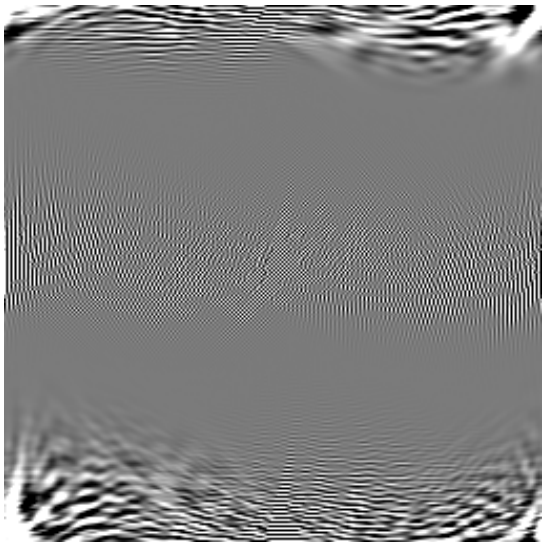

Wigner function of a wavepacket for kicked rotator, $K = 0.9$.

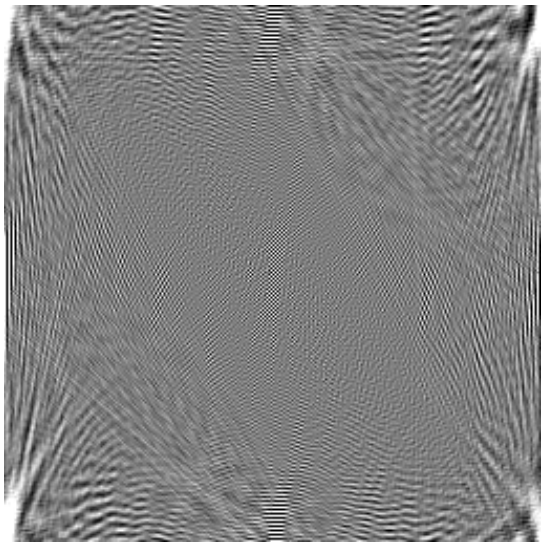

Wigner function of a wavepacket for kicked rotator, $K = 2$.

Wigner function on a quantum computer: algorithm I

C. Miquel, J. Paz, M. Saraceno, E. Knill, R. Laflamme, C. Negrevergne, Nature 418, 59 (2002): Measures Wigner function at **one given location** using an ancilla qubit.

1) Apply one Hadamard gate to the ancilla qubit

2) Apply $A(\Theta, n) = S^{\Theta} R V^{-n} \exp(2i\pi\Theta n/2N)$ to the system **conditioned** by the value of the ancilla qubit (S=shift in Θ basis, $S(|\Theta\rangle) = |\Theta + 1\rangle$; V=shift in the n basis; R=reflection operator, $R(|n\rangle) = |N - n\rangle$)

3) Apply one Hadamard gate to the ancilla qubit

Expectation value of the ancilla: $\langle\sigma^z\rangle = Re[Tr(U(\Theta, n)\rho)] = 2NW(\Theta, n)$ (ρ is the density matrix and $N = 2^{n_q}$ is the dimension of the Hilbert space).

Problem: values of W are very small, and **require exponentially many iterations**.

Wigner function on a quantum computer: algorithm II

M. Terraneo, B. Georgeot and D. Shepelyansky, Phys. Rev. E 71, 066215 (2005): builds a state whose amplitudes in a chosen basis gives the Wigner function.

1) Transform $|\psi_0\rangle|\psi_0\rangle$; into $|U^t\psi_0\rangle|U^t\psi_0\rangle = \sum_{\theta,\theta'} \psi(\theta)\psi^*(\theta')|\theta\rangle|\theta'\rangle$. Then add an extra qubit, transform into $\sum_{\theta,\theta'} \psi(\theta)\psi^*(\theta')|\theta+\theta'\rangle|\theta'\rangle$ (addition)

2) Fourier transform of second register $\Rightarrow \sum_\Theta \sum_n (\sum_{\theta'} e^{-\frac{2i\pi}{N}n\theta'}\psi(\Theta-\theta')\psi^*(\theta'))|\Theta\rangle|n\rangle = 2\sqrt{N}\sum_\Theta \sum_n W(\Theta,n)e^{-\frac{2i\pi}{N}n\Theta/2}|\Theta\rangle|n\rangle$ where $\Theta = \theta+\theta'$ and Θ varies from 0 to $2N-1$ and n from 0 to $N-1$.

3) Add an extra qubit in the state $|0\rangle$, apply Hadamard gate and multiply by the phases $e^{-\frac{2i\pi}{N}n\Theta/2}$ and $e^{-\frac{2i\pi}{N}(n-N)\Theta/2}$ $\Rightarrow$ $|\psi_f\rangle = \sqrt{2N}\sum_{\Theta=0}^{2N-1}\sum_{n=0}^{2N-1} W(\Theta,n)|\Theta\rangle|n\rangle$

Allows **further data treatment** (amplitude amplification, wavelet transform).

Amplitude amplification

(Brassard, Hoyer, Mosca, Tapp, quant-ph/0005055)

$\Rightarrow$ Generalization of Grover's algorithm. Amplitude amplification increases the amplitude of a **whole subspace** H.

$\Rightarrow$ Let P be a projector on this subspace H and $\hat{V}$ an operator taking $|0\rangle$ to a state having some projection on H. Repeated iterations of $\hat{V}(I - 2|0\rangle\langle 0|)\hat{V}^{-1}(I - 2P)$ on $\hat{V}|0\rangle$ will increase the projection. Indeed, if one write $\hat{V}|0\rangle = P\hat{V}|0\rangle + (I - P)\hat{V}|0\rangle$, the result of one iteration is to **rotate the state toward** $P\hat{V}|0\rangle$ **staying in the subspace spanned by** $P\hat{V}|0\rangle$ **and** $(I - P)\hat{V}|0\rangle$. One can check that after one iteration the state has a component along $(I - P)\hat{V}|0\rangle$ decreased by an amount which depends on $|P\hat{V}|0\rangle|^2$

$\Rightarrow$ If N is dimension of total Hilbert space and M the dimension of H, $\sqrt{N/M}$ **iterations needed to bring the probability to be in** H **close to** 1.

Wavelet transforms

$\Rightarrow$ Wavelet transforms = generalizations of Fourier transform. Wavelet bases: each basis vector is **localized in position as well as momentum**, with **different scales** ($\neq$ Fourier basis = plane waves).

$\Rightarrow$ Basis vectors are obtained by translations and dilations of an original function and their properties enable to probe the different scales of the data as well as localized features, both in space and frequency.

$\Rightarrow$ Wavelet transforms are used in a **large number of applications** involving classical data treatment, in particular they allow to reach large compression rates for classical images in standards like MPEG.

$\Rightarrow$ **Efficient quantum algorithms** for implementing such transforms have been built, requiring polynomial resources to treat an exponentially large vector.

Wigner function on a quantum computer: measurements

Numerical results for kicked rotator on a N dimensional space after t iterations:

1) **Direct measurements:** $\Rightarrow$ quantum algorithm $O(tN^{\alpha})$ with $\alpha \approx 1.8 - 2$; classical $O(tN^2 \log N)$ $\Rightarrow$ **Small polynomial gain**

2) Coarse-grained measurement $\Rightarrow$ **possible exponential gain**

3) Amplitude amplification on a $N_D \times N_D$ square: $O(tN + N_D N)$ classically, $O(tN_D^{\alpha} N)$ quantum $\Rightarrow$ **Small polynomial gain**

4) Wavelet transformed: $O(tN^{\beta})$ with $1.4 \leq \beta \leq 2$ quantum, $O(tN^2 \log N)$ classical $\Rightarrow$ **Larger polynomial gain**

Gain is larger in chaotic regime

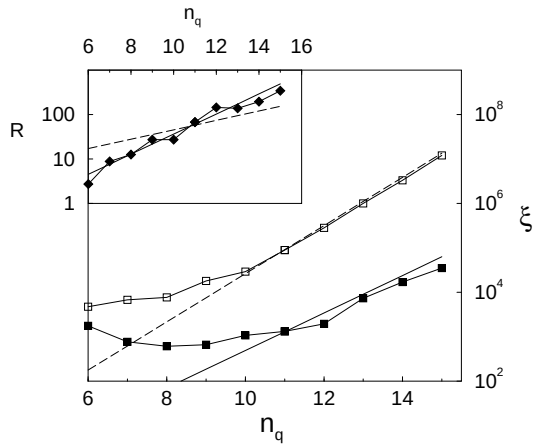

$1/(\sum N^2 W(\Theta, n)^4)$ for Wigner function (open squares) and wavelet transform of it (full squares) for $K = 2$. Straight lines are resp. $\alpha = 1.8$ and $\beta = 1.4$.

Husimi function on a quantum computer

Husimi function: **J. P. Paz, A. J. Roncaglia and M. Saraceno, Phys. Rev. A 69, 032312 (2004).**

$\rho_H(\theta_0, n_0) = |\langle\phi_{(\theta_0,n_0)}|\psi\rangle|^2$ where $\phi_{(\theta_0,n_0)}(\theta, n) = A\sum_n e^{-(n-n_0)^2/4a^2 - i\theta_0 n}|n\rangle$ is a Gaussian coherent state centered on (θ_0, n_0) with width a (A is a normalization constant). Construct a Gaussian using ground state of Harper Hamiltonian.

Much simpler: modified Husimi function: **K. M. Frahm, R. Fleckinger and D. L. Shepelyansky, Eur. Phys. J. D 29, 139 (2004).**

$\rho_H^{(p)}(\theta_0, n_0) = |\langle\phi^{(p)}_{(\theta_0,n_0)}|\psi\rangle|^2$ where $\phi^{(p)}_{(\theta_0,n_0)}(\theta, n) = (1/N^{1/4})\sum_{n=n_0}^{n_0+\sqrt{N}-1} e^{-i\theta_0 n}|n\rangle$

Quantum Fourier transform to first half of the qubits: $\psi \Rightarrow |\psi_H\rangle = \sum_{\theta,n} H(\theta, n)|\theta\rangle|n\rangle$ where θ and n take only $\sqrt{N}$ values each and $|H(\theta, n)|^2$ is the modified Husimi function.

Modified Husimi function: measurements

Numerical results for kicked rotator on a N dimensional space after t iterations:
1) Husimi function $O(tN^{\gamma})$ with $0.5 \leq \gamma \leq 0.7$; classical $O(tN) \Rightarrow$ **Polynomial gain** for direct measurements
2) Coarse-grained measurement $\Rightarrow$ **possible exponential gain**
3) Amplitude amplification on a $N_D \times N_D$ square: $O(t\sqrt{N}N_D^{\gamma-1/2})$ quantum, $O(tN)$ classical $\Rightarrow$ **Polynomial gain**, independent of system
4) Wavelet transform $\Rightarrow$ **Polynomial gain**
Figure: modified Husimi function of kicked rotator for $K = 0.9$ (top) and $K = 2$(bottom)

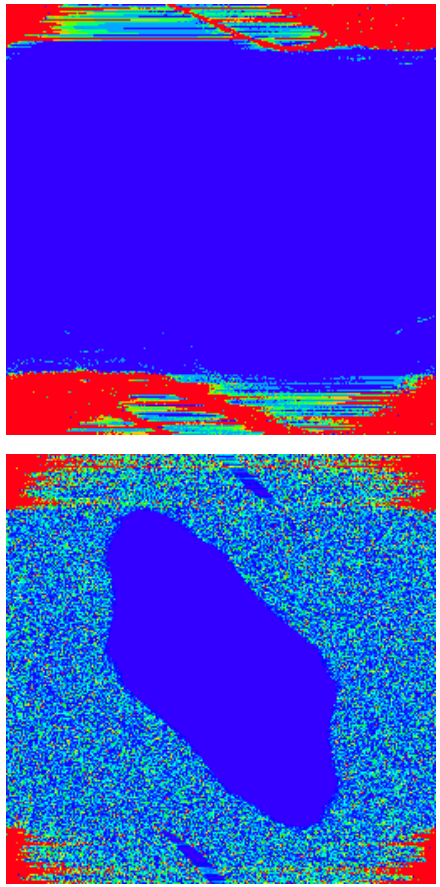

Standard images

Numerical simulations $\longrightarrow$ wavelet transform is **very efficient** at compressing information for standard images

Largest wavelet coefficients can be obtained in **polynomial time** for **exponentially** large images. **Total gain** depends on efficiency of encoding the image

But reconstruction of image from such largest wavelet coefficients leads to large loss of information

Spectrum: phase estimation

A. Kitaev, quant-ph/9511026, D. Abrams and S. Lloyd, Phys. Rev. Lett. 83, 5162 (1999): Given an unitary operator U and an eigenvector $|u\rangle$, find efficiently the associated eigenvalue $e^{2i\pi\omega_u}$.

- Start from $1/\sqrt{N}\sum_{t=0}^{N-1}|t\rangle|u\rangle$
- Transform it into $1/\sqrt{N}\sum_{t=0}^{N-1}|t\rangle|U^t u\rangle = 1/\sqrt{N}\sum_{t=0}^{N-1}e^{2i\pi\omega_u t}|t\rangle|u\rangle$
- Quantum Fourier transform of first register $\Rightarrow |\omega_u\rangle|u\rangle$

Problem: needs i) an operator U whose exponentially large iterates are **efficiently implementable** and ii) a good approximation of one eigenvector

Note: Shor's algorithm can be reinterpreted as phase estimation on the operator $U|y\rangle = |ay \bmod(N)\rangle$

Spectrum: phase estimation + Grover

Works if i) and ii) are not fulfilled; evolution operator should be efficiently implementable.

- Start with $\sum_{t=0}^{N-1} |t\rangle|\psi_0\rangle$, for example $|\psi_0\rangle = 2^{-nq} \sum_n |n\rangle$
- Transform it into $2^{-nq} \sum_{t=0}^{N-1} |t\rangle|U^t\psi_0\rangle$ in $O(N)$ operations,
- QFT of the first register $\Rightarrow$ peaks centered at eigenvalues of U
- Measurement of the first register $\Rightarrow$ one eigenvalue of U with good probability in $O(N)$ operations
- Amplitude amplification (Grover): all eigenvalues in a given interval in $O(N\sqrt{N})$ operations.

Compare with $O(N^2)$ operations classically (kicked Harper), $O(N^3)$ (general system)

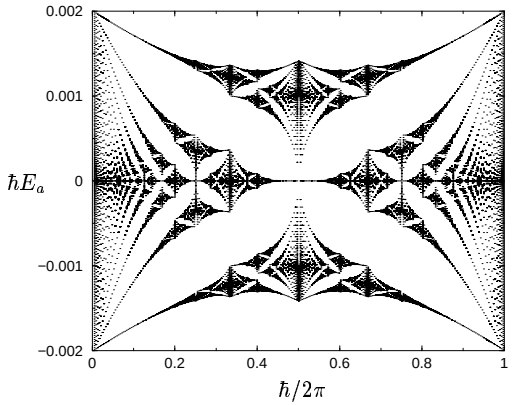

fractal spectrum (Harper model)

Concluding remarks

- Quantum maps: especially simple dynamics, yet complex behaviour
- Adapted to small-size quantum computers; some of them already implemented.
- At least polynomial gain can be obtained; possibly exponential
- Have inspired pseudorandom operators, which can produce efficiently quasi-random vectors on quantum computers (J. Emerson, Y. Weinstein, M. Saraceno, S. Lloyd and D. Cory, Science **302**, 2098 (2003)).

Simulating classical chaos

(B. Georgeot and D. Shepelyansky, Phys. Rev. Lett. 86, 5393 (2001))

Arnold cat map:

$\bar{y} = y + x \pmod 1$

$\bar{x} = y + 2x \pmod 1$

Textbook example of hard chaos.

Classical exponential instability $\Rightarrow$ hard to simulate for long times.

Phase-space density on a $2^n \times 2^n$lattice:

classical computation: one iteration $\Rightarrow$ 2^{2n+1} additions

quantum computation: one iteration $\Rightarrow$ $16n - 22$ quantum gates

"Arnold-Schroedinger cat"

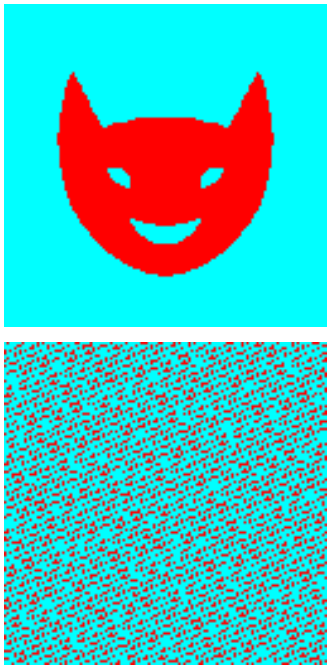

10 iterations of the cat map

Quantum algorithm:

To simulate phase-space density on a $2^n \times 2^n$lattice:

- **Step I** Preparation of initial wavefunction: $\psi(0) = \sum_{i,j} a_{i,j}|x_i\rangle|y_j\rangle$

- **Step II** Modular addition

  $\sum_{i,j} a_{i,j}|x_i\rangle|y_j\rangle \Rightarrow \sum_{i,j} a_{i,j}|x_i\rangle|y_j + x_i(\mathrm{mod}(1))\rangle = \sum_{i,j} b_{i,j}|x_i\rangle|y_j\rangle$

- **Step III** Modular addition

  $\sum_{i,j} b_{i,j}|x_i\rangle|y_j\rangle \Rightarrow \sum_{i,j} b_{i,j}|x_i + y_j(\mathrm{mod}(1))\rangle|y_j\rangle = \sum_{i,j} c_{i,j}|x_i\rangle|y_j\rangle$

only $16n - 22$ quantum gates per iteration; needs $3n - 1$ qubits

Strange attractors

$\Longrightarrow$ Dissipative dynamical systems often converge to **strange attractors**

$\Longrightarrow$ They are characterized by **fractal dimensions** and **chaotic unstable** dynamics of trajectories

$\Longrightarrow$ Applications: turbulence and weather forecast, molecular dynamics, chaotic chemical reactions, multimode solid state lasers, ecology and physiology, etc...

Strange attractors: examples

Lorenz attractor (1963):

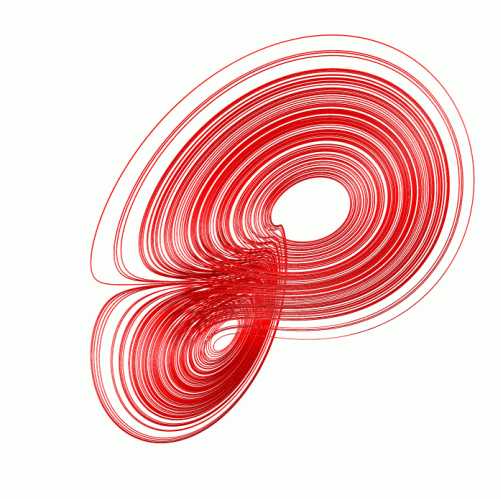

Hénon attractor (1976):

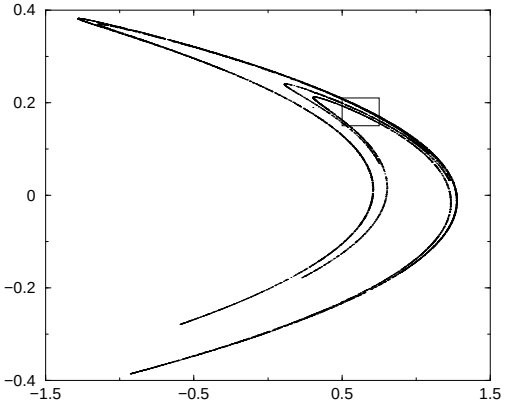

Simulating strange attractors

(M.Terraneo, B.Georgeot and D. Shepelyansky, Eur. Phys. J. D 22, 127 (2003)).

dissipative deterministic map:

$\bar{y} = \frac{y}{2} + x \pmod 2 \quad , \quad \bar{x} = \frac{y}{2} + 2x \pmod 1$

Converges to a **strange attractor** of **fractal dimension** ≈ 1.543.

Quantum computation of a density on a $2^n \times 2^{n+1}$ lattice:

one iteration $\Rightarrow 17n - 10$ **quantum gates**

Four registers $|x\rangle, |y\rangle, |\text{workspace}\rangle, |\text{garbage}\rangle$

Garbage register is needed due to **irreversibility** of the map

Size of garbage grows like t **(simplest algorithm) or** $\ln t$ **(pebble game)**

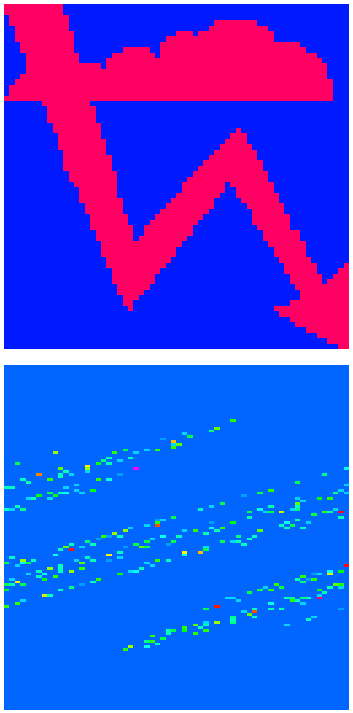

10 iterations of the map

Extracting information

- to obtain the full phase space density requires an **exponential** number of measurements: how to extract information efficiently?

- Fourier coefficients of the discretized phase space density: apply **Quantum Fourier transform** after iterating the map; **possibility of exponential gain.**

- **Large harmonics** $\longrightarrow$ **exponentially small scales** very quickly populated due to chaos.

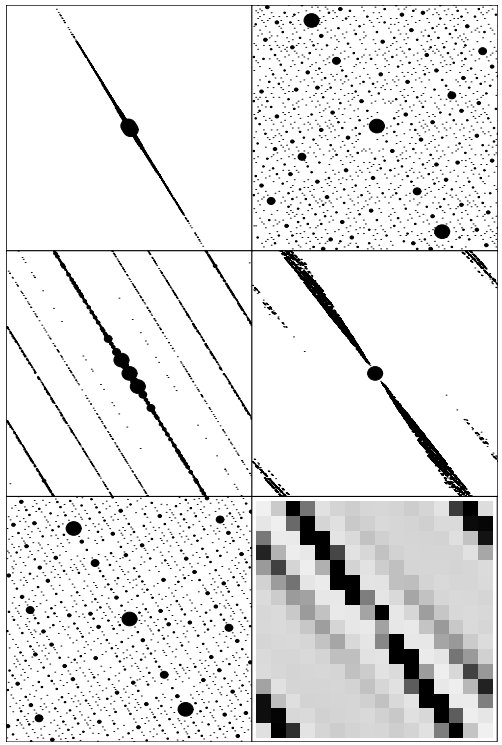

Figure: Fourier coefficients for the cat map and a modified cat map.

Extracting information II

- For attractor: **Spectrum of phase space correlation functions:**

$$C(t, k_{x,y}) = \sum e^{(2i\pi(x(t,x_0)+y(t,x_0)))} e^{2i\pi(k_x x_0 + k_y y_0))}$$

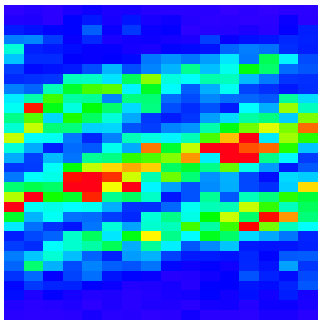

- Needs $O(n^2)$ gates (t iterations of the map + $2n+1$ one-qubit rotations + t reverse iterations + Quantum Fourier Transform). Measure only the first n_f qubits $\rightarrow$ polynomial number of measurements gives **coarse grained image** of $|C(t, k_{x,y})|^2$ (see example left on top)

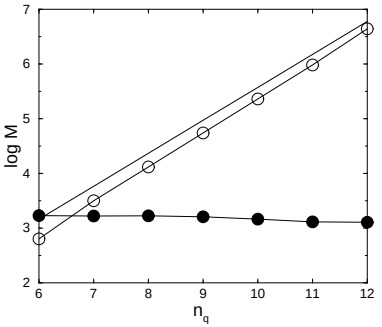

- **Possibility of exponential gain**; numerics: exponentially faster than classical Monte-Carlo (figure left bottom: open circle: Monte-Carlo, full circle: quantum algorithm)

Poincaré recurrences/periodic orbits

(B. Georgeot, Phys. Rev. A 69, 032301 (2004))

Other way to extract information

- For classical bounded conservative systems

  Theorem of Poincaré $\longrightarrow$ some points from an arbitrary small phase space domain A will eventually come back to A. $\Rightarrow$ recurrence times. Very long times, hard to find numerically

- For more general systems: periodic orbits: orbits which come back exactly to their starting position in phase space. "Backbone" of classical dynamics

  $\longrightarrow$ Enable to compute diffusion coefficients, properties of strange attractors

  $\longrightarrow$ Enter classical and semiclassical trace formulas

Arnold Cat map

$\bar{y} = y + x \pmod 1$, $\bar{x} = y + 2x \pmod 1$

action of the 2×2 matrix $L = \begin{pmatrix} 2 & 1 \\ 1 & 1 \end{pmatrix}$ on $\begin{pmatrix} x \\ y \end{pmatrix}$

periodic points = rational points $\rightarrow$ they all belong to some $g \times g$ lattice of $\{(p_1/g, p_2/g)\}$, $p_1, p_2 = 0, 1...g$

On such lattice, the map acts on numerators only as $\bar{y} = y+x \pmod g$, $\bar{x} = y + 2x \pmod g$, or $\begin{pmatrix} \bar{x} \\ \bar{y} \end{pmatrix} = L \begin{pmatrix} x \\ y \end{pmatrix} \pmod g$, with $x, y, \bar{x}, \bar{y}$ integers

Lattice period function $\alpha(g)$= smallest integer such that after $\alpha(g)$ iterations all points in the lattice have come back to the initial position

$\alpha(g)$=smallest integer t such that $L^t = I \pmod g$

$\alpha(g)$

$\alpha(g)$= very erratic function of g, of order g

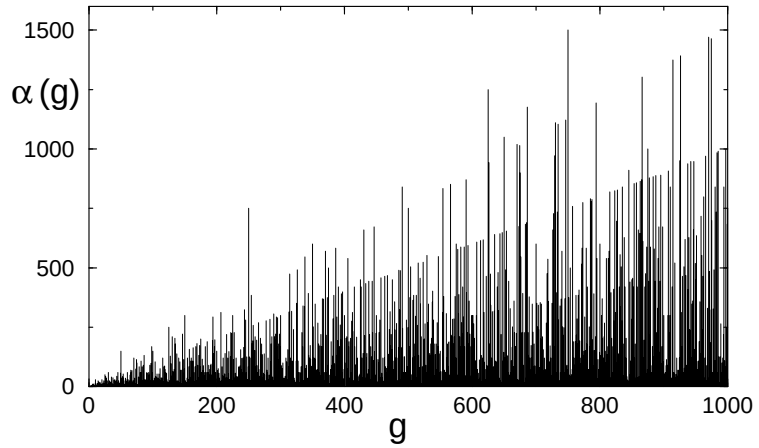

The lattice period function $\alpha(g)$ for the Arnold cat map.

Quantum computing $\alpha(g)$

- Start with $N^{-1/2}\sum_{t=0}^{N-1}|t\rangle|1\rangle|0\rangle|0\rangle|1\rangle$ where $N=2^{n_q}$ with $n_q \sim \log_2 g$
- Transform it into $N^{-1/2}\sum_{t=0}^{N-1}|t\rangle|A_t\rangle|B_t\rangle|C_t\rangle|D_t\rangle$

  where (A_t, B_t, C_t, D_t) are entries of matrix L^t mod g, periodic function of t
- Measure the last registers. Result: $|A\rangle|B\rangle|C\rangle|D\rangle$corresponding to matrix K. Total state: $M^{-1/2}\Sigma_{j=0}^{M-1}|t_j\rangle|A\rangle|B\rangle|C\rangle|D\rangle$ where t_j are all t such that $L^{t_j}=K$, and $M\approx 2^{n_q}/\alpha(g)$.
- Fourier Transform first register $\longrightarrow$ peaks at multiples of $M\approx 2^{n_q}/\alpha(g)$.

  In total $O((\log g)^3)$ operations and $\sim 9\log g$ qubits

  very similar to Shor algorithm

Period r of a function

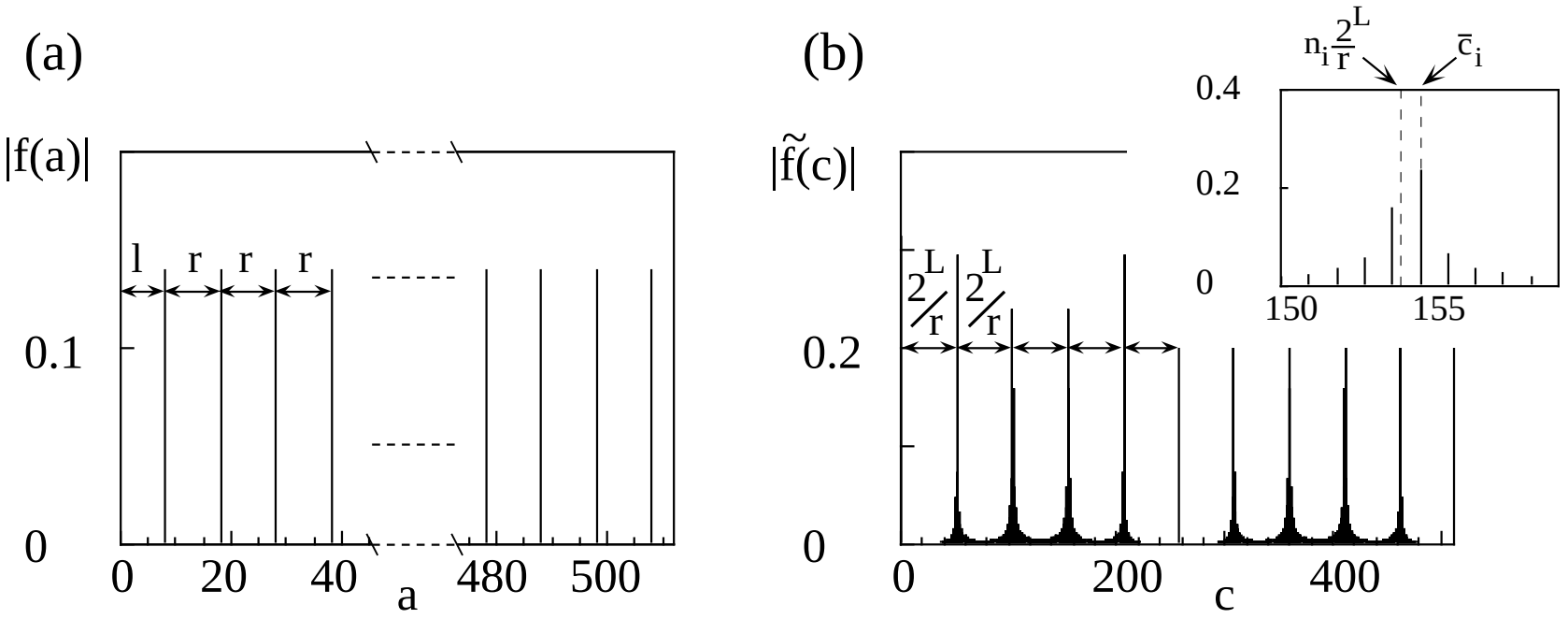

From Barenco et al., Phys Rev A **54**, 139 (1996)

More generally

-start from an initial point and look for periodicities of its iterates

-use discretized (unitary) map on a lattice $x_i = i/N,\ i = 0, ..., N-1$ and $y_j = j/N,\ j = 0, ..., N-1$, with $N = 2^{n_q}$

-initial state $2^{-p/2} \sum_{t=0}^{2^p-1} |t\rangle|x_0\rangle|y_0\rangle$ with $p \approx n_q$

-transform efficiently to $2^{-p/2} \sum_{t=0}^{2^p-1} |t\rangle|L^t(x_0)\rangle|L^t(y_0)\rangle$

-Quantum Fourier transform the first register

-Efficient if fast (polynomial) classical computation of (L^{2^k}) is possible

If it does not work

-**iterates of** L are **not** efficiently computable, but L efficiently computable (often the case)

-choose a time t fixed and a subdomain A; simple case: square of size $P \times P$ with $P = 2^p$ in phase space of size $N \times N$ where $N = 2^{n_q}$

-initial state is $|\psi_0\rangle = 2^{-p} \sum_{i=0}^{2^p-1} \sum_{j=0}^{2^p-1} |x_i\rangle|y_j\rangle$

-$|\psi_0\rangle \rightarrow 2^{-p} \sum_{i=0}^{2^p-1} \sum_{j=0}^{2^p-1} |L^t(x_i)\rangle|L^t(y_j)\rangle$

-give a (-1) phase to the values of $|L^t(x_i)\rangle|L^t(y_j)\rangle$ ending a trajectory returning to A, then invert everything $\rightarrow 2^{-p} \sum_{i=0}^{2^p-1} \sum_{j=0}^{2^p-1} \epsilon|x_i\rangle|y_j\rangle$, where $\epsilon = \pm 1$

-use this as **an oracle in Grover iterations;** one return among M is found in $O(tP/\sqrt{M})$ operations, as opposed to $O(tP^2/M)$ classically

Periodic orbits

-one can also obtain **periodic orbits** of period t

-start from all the $N \times N$ points of the lattice with $N = 2^{n_q}$

-$|\psi_0\rangle \rightarrow 2^{-n_q} \sum_{i=0}^{2^{n_q}-1} \sum_{j=0}^{2^{n_q}-1} |x_i\rangle|y_j\rangle|L^t(x_i)\rangle|L^t(y_j)\rangle$

-after t iterations the value of the iterate is compared to the initial value; a minus sign is given if it is the same;then invert the process

$\rightarrow 2^{-n_q} \sum_{i=0}^{2^{n_q}-1} \sum_{j=0}^{2^{n_q}-1} \epsilon|x_i\rangle|y_j\rangle$

-use this as **an oracle in Grover iterations;** one periodic orbit among M is found in $O(tN/\sqrt{M})$ operations, as opposed to $O(tN^2/M)$ classically

Examples

Classical maps of the form: $\bar{n} = n - kV'(\theta)(\text{mod } 2\pi L)$; $\bar{\theta} = \theta + T\bar{n}(\text{mod } 2\pi)$

-$V(\theta) = \cos\theta$: **Chirikov standard map;** discretized map on a $2^{n_q} \times 2^{n_q}$ lattice can be performed in $O(n_q^3)$ gates $\rightarrow$ **quadratic gain**

-$V(\theta) = -\theta^2/2$: **sawtooth map;** discretized mapping: $\bar{Y} = Y + [NK(2\pi X/N - \pi)/(2\pi)](\text{mod}N)$; $\bar{X} = X + \bar{Y}(\text{mod}N)$

integer $K\rightarrow$ **exponential gain**

non integer $K\rightarrow$ **quadratic gain**

$K = \pm 1/2$ for return times $\rightarrow$ only 3 registers

domain 4×4 in a 8×8 lattice$\rightarrow$ only 8 qubits

Discretized vs continuous system

-It is known that discretized unitary maps can be built for any area-preserving maps; they can be studied for their own's sake.

-Periodic orbits found are exact periodic orbits of the discretized systems

-Shadowing theorem (hyperbolic systems): an exact trajectory will remain close to the dynamics of each discretized point for arbitrary times.

$\Rightarrow$ Results of the algorithms above are **Poincaré recurrence times** of the continuous system.

Concluding remarks

- Quantum computers can solve problems of classical chaos
- Gain depends on the system and the quantity considered
- More work to be done...